Research on Engineering Structures & Materials

journal homepage: http://jresm.org

Research Group

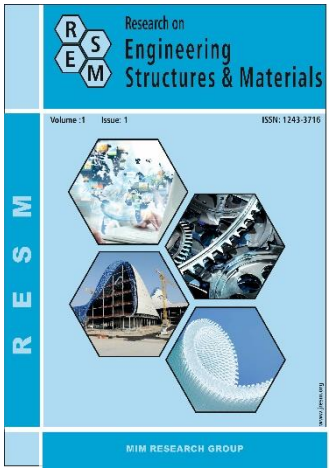

Natural frequencies, modes and critical velocities of top tensioned cantilever pipes conveying pressurized steady two-phase flow under thermal loading

Adeshina S. Adegoke, Ayo A. Oyediran

Online Publication Date: 14 Feb 2018
URL: http://dx.doi.org/10.17515/resm2017.16en0301
DOI: http://dx.doi.org/10.17515/resm2017.16en0301

Journal Abbreviation: *Res. Eng. Struct. Mat.*

To cite this article
Adegoke AS, Oyediran AA. Natural frequencies, modes and critical velocities of top tensioned cantilever pipes conveying pressurized steady two-phase flow under thermal loading. *Res. Eng. Struct. Mat*., 2018; 4(4-): 297-323.

Research on
Engineering
Structures & Materials
journal homepage: http://jresm.org

RESEARCH
GROUP

Research Article

Natural frequencies, modes and critical velocities of top tensioned cantilever pipes conveying pressurized steady two-phase flow under thermal loading

Adeshina S. Adegoke, Ayo A. Oyediran*

Department of Mechanical Engineering, University of Lagos, Nigeria

Article Info

Article history:
Received 1 Mar 2017
Revised 14 Sep 2017
Accepted 16 Nov 2017

Keywords:
Hamilton's principle,
Cantilever pipe conveying two-phase flow,
Critical velocity,
Natural frequency,
Multiple scale perturbation technique

Abstract

This paper studied the planar dynamics of top tensioned cantilevered pipes conveying pressurized steady two-phase flow under thermal loading. The governing equations of motions were derived based on Hamilton's principle, the centerline is assumed to be extensible in order to account for possible thermal expansion; resulting to a set of coupled axial and transverse partial differential equations. Analytical approach was used to resolve the governing equations using the multiple scale perturbation technique, which aided the development of theoretical schemes for estimating the natural frequencies and mode shapes. Numerical results were presented for a case study of two phase flow of water and air with the stability and dynamic behavior of the system studied linearly via Argand diagrams which were constructed as the mixture flow velocity is increased for various void fractions. The Argand diagram assessment of the axial vibration natural frequencies shows that the attainment of the critical velocity is delayed for a cantilever pipe conveying two phase flow compared to when the pipe is conveying single phase flow. The result of the linear analysis of the transverse vibration reveals that at the critical mixture velocity, the system loses stability through Hopf bifurcation. Similarly, to the axial vibration, the attainment of the critical velocity was observed to be at higher velocities for a cantilever pipe conveying two phase flow as compared to when the pipe is conveying single phase flow. In addition to, the critical velocity is observed to be increasing as the void fraction of the two phase flow increases. The assessment of the effect of thermal loading, pressurization and top tension on the attainment of the critical velocity shows that thermal loading, pressurization and compression at the tip hastens the attainment of the critical velocity while tensioning top tension delays the attainment of the critical velocity.

1. Introduction

Instability of pipes conveying fluid are mainly of two different cases, the first is as a result of the unstable vibration caused by the fluid flow when the flow velocity surpasses a critical value and the other is a vibration due to oscillating fluid flow (Pulsating Flows). Vast publications exist on the study of the effect of internal flow on the dynamics of cantilever pipes, with most of the earlier work focusing on the linear dynamics of the pipe emphasizing on the determination of the critical velocity for the onset of flutter [1-5] for a single phase fluid. Sequel to these works, the nonlinear dynamics of pipes captivated the minds of many curious researchers which resulted to various publications on the subject; notable among these is the detail theoretical work by Semler et al [6] where a

*Corresponding author: ayooyediran@hotmail.com
DOI: http://dx.doi.org/10.17515/resm2017.16en0301

comprehensive nonlinear equation was derived for a cantilever pipe based on inextensible theory. However, existing publications on the dynamics of fluid-conveying cantilevered pipes taking into account extensibility is rare with the pioneering work by Ghayesh et al [7], where he studied the nonlinear dynamics of cantilevered extensible pipe conveying single phase fluid without thermal loading, he observed that conversely to inextensible pipe, an extensible pipe elongates in the axial direction as the flow velocity increases.

The combined thermal and pressurization effect on the instability of pipes is not an area with vast historical research trends. However, recent findings on the contributions of transient temperature to pipe walking prompted some studies on this subject, Qian et al. [8], studied the instability of simply supported pipes conveying fluid under thermal loads and discovered that the critical fluid velocity decreases with increasing temperature. Another interesting result of Marakala et al [9] reveals that the frequency of vibration increases with increase in pressure and decreases with increase in temperature. The increase in pressure increases the velocity of the fluid flow and reduces the damping effect. Temperature has an effect on displacement as well as frequency, since thermal contraction and expansion increases due to high heat transfer rate at high velocity. As the temperature of the fluid increases, the frequency decreases due to softening effect of tube. However, these publications were on the dynamics of a simply supported pipe.

Two phase flow is a common flow phenomenon in various industrial pipes, but very few publications exist on the instability behavior of pipes conveying two phase flow. Miwa et al [10] did an in-depth review of the extent of existing work on two-phase flow induced vibrations, stating that there exist very few researches on the instability behavior of pipes due to internal two phase flow. In his review, Miwa et al explains that internal two phase flow induced vibration can be initiated by various hydrodynamic phenomena, depending on the geometrical configurations of the flow channels and operating conditions, gas-liquid two phase flow may create vibrations with various modes of amplitude and frequency. Young and Qiang [11] highlighted that in gas and liquid transportation, the gas and the liquid normally do not travel at the same velocity in the pipeline because of difference in viscosities, for an upward flow in a vertical pipe, the gas phase will flow at higher velocity than the liquid because it is denser and less viscous while in a downward flow, the gas is slower as a result of variation in densities. Monette and Pettigrew [12] presents an excellent experimental paper on the fluidelastic instability of flexible tubes subjected to two-phase flow which might be one of the premier paper on the dynamics of pipe conveying two phase flow, where experimental results were compared with the theoretical estimations and also reveals the relationship between the void fraction and the dynamics of the pipe for a two phase liquid-gas flow.

Majority of the existing publications focused on single phase flow, not many considered thermal effect, and most of the existing equations of motion for cantilever pipe conveying fluids are based on the inextensible theory. However, there seems to be some gaps on the study of combined effect of Multiphase flow and thermal effect on the dynamics of cantilever pipes conveying fluids. This present study investigates the dynamics of top tensioned cantilever pipes conveying pressurized steady two-phase flow under thermal loading. Approximate analytical approach is used to resolve the governing equations by imposing the method of multiple scales perturbation technique directly to the systems equations (direct-perturbation method).

2. Problem Formulation and Modelling

Considering a system of cantilever cylindrical pipe of length (L), having a cross-sectional area (A), mass per unit length (m_p) and flexural rigidity (EI), conveying multiphase flow, and flowing parallel to the pipe's center line.

The center line axis of the pipe in its undeformed state is assumed to overlaps with the Y axis and the cylinder is assumed to vibrate in the (Y, X) plane (see fig. 1). To derive the system's governing equations of motion, the following basic assumptions were made for the cylinder and the fluid: (i) the mean flow velocity is constant; (ii) the cylinder is slender, so that the Euler–Bernoulli beam theory is applicable; (iii) although the deflections of the cylinder may be large, the strains are small; (iv) the cylinder centreline is extensible.

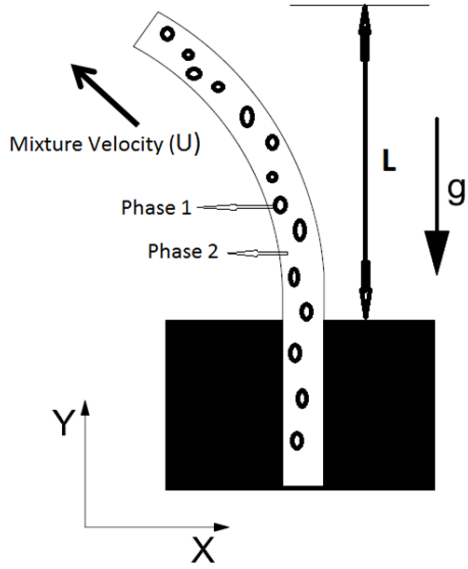

Fig. 1 System's Schematics

The centerline of the cantilever pipe is assumed extensible so as to account for possible expansion due to the high temperature of the fluid content. Semler et al [6] expressed the geometric relation of the centerline of an extensible pipe as:

$$1 + \epsilon(\mathrm{Y}) = \sqrt{\left[1 + \frac{\partial \mathrm{u}}{\partial \mathrm{Y}}\right]^2 + \left[\frac{\partial \mathrm{v}}{\partial \mathrm{Y}}\right]^2} \tag{1}$$

$\epsilon(\mathrm{Y})$ is the axial strain along the pipe's centerline.

Assuming θ to be the angle between the pipe's centerline and the Y- axis, this can be defined as:

$$\cos\theta = \frac{1 + \partial \mathrm{u}/\mathrm{dY}}{1 + \epsilon(\mathrm{Y})}, \qquad \sin\theta = \frac{\partial \mathrm{v}/\mathrm{dY}}{1 + \epsilon(\mathrm{Y})} \tag{2}$$

The curvature k is related to the geometry as:

$$\mathrm{k} = \frac{1}{1 + \epsilon}\frac{\partial \theta}{\partial \mathrm{Y}} \tag{3}$$

The derivative in Eq. (3) can be obtained from Eq. (2) as:

$$\frac{\partial\theta}{\partial Y}=\frac{\left[\frac{\partial^2 v}{\partial Y^2}\left(1+\frac{\partial u}{\partial Y}\right)-\frac{\partial v}{\partial Y}\frac{\partial^2 u}{\partial Y^2}\right]}{(1+\epsilon)^2} \tag{4}$$

The second derivative is expressed adopting Lagrange notations as:

$$\left(\frac{\partial\theta}{\partial Y}\right)^2 = v''^2-2v''^2u'-2v''^2u''^2-2v'v''u'' \tag{5}$$

2.1. Derivation of the Equation of Motion

The equations of motion are derived using the energy method. The energy method is based on the Hamilton's principle, which is defined as the variations of the time derivative of the Lagrangian. This can be mathematically expressed as:

$$\delta\int_{t1}^{t2}\mathcal{L}\,dt=\int_{t1}^{t2}\sum_{j=1}^{n}M_jU_j\left(\dot{r}_L+\sum_{j=1}^{n}U_j\tau_L\right)\delta r_L\,dt, \tag{6}$$

Where

n is the number of phases in the fluid, which will be 2 for a two phase flow

M_j is the mass of the phases in the fluid

U_j is the flow velocity of the phases in the fluid

$\mathcal{L}$ is the Lagrangian operator which is expressed as:

$$\mathcal{L}=\mathcal{T}_f+\mathcal{T}_p-\mathcal{V}_f-\mathcal{V}_{p,} \tag{7}$$

$\mathcal{T}_p$ and $\mathcal{V}_p$ are the kinetic and potential energies of the pipe, and $\mathcal{T}_f$ and $\mathcal{V}_f$ are the kinetic and potential energies associated with the conveyed fluid.

The following expressions hold:

$\dot{r}_L=\dot{u}_Li+\dot{v}_Lk$ and $\tau_L=u'_Li+v'_Lk$

2.1.1. Kinetic Energy

The total kinetic energy of the system is the summation of the kinetic energy of the pipe and the kinetic energies of the phases/components of the flowing fluid.

The velocity vector of the pipe's centerline is expressed as:

$$\vec{V}_p=\frac{\partial u}{\partial t}\hat{i}+\frac{\partial v}{\partial t}\hat{j} \tag{8}$$

Therefore, the kinetic energy of the pipe is expressed as:

$$\mathcal{T}_p=\frac{1}{2}m_p\int_0^L\left[\left(\frac{\partial u}{\partial t}\right)^2+\left(\frac{\partial v}{\partial t}\right)^2\right]dx \tag{9}$$

As illustrated by Semler et al [6], the axial elongation of the pipe is complemented by a lateral contraction, due to the Poisson effect. This will impact the flow velocity of the fluid phases/components such that:

$$\sum_{j=1}^{n} U_j = [(1+\epsilon)/(1+a\epsilon)] \sum_{j=1}^{n} U_{0_j} \tag{10}$$

Where U_{0_j} and U_j are the flow velocities before and after elongation, the subscript (j) is used to identify the various phases/components of the conveyed fluid, (ϵ) is the axial strain and (a) relates to the Poisson ratio (v) as $a = 1 - 2v$; for an extreme case $v = 0.5$ and a becomes zero Ghayesh [7].

The flow velocity relative to the centerline axis of the pipe is expressed as:

$$\vec{V}_f = \left\{\frac{\partial u}{\partial t} + \sum_{j=1}^{n} U_j(1-a\epsilon)\left(1+\frac{\partial u}{\partial x}\right)\right\}\hat{\imath} + \left\{\frac{\partial v}{\partial t} + \sum_{j=1}^{n} U_j(1-a\epsilon)\left(\frac{\partial v}{\partial x}\right)\right\}\hat{\jmath} \tag{11}$$

Therefore, the Kinetic energy of the conveyed fluid is expressed as:

$$\mathcal{T}_f = \frac{1}{2}\sum_{j=1}^{n} M_j \int_0^L \left\{\left(\frac{\partial u}{\partial t}\right)^2 + \left(\frac{\partial v}{\partial t}\right)^2 + U_j{}^2\left[1 + 2\frac{\partial u}{\partial x} + \left(\frac{\partial u}{\partial x}\right)^2 - 2a\left(\frac{\partial u}{\partial x} + \frac{1}{2}\left(\frac{\partial v}{\partial x}\right)^2\right) + \left(\frac{\partial v}{\partial x}\right)^2\right] + 2U_j\left[\frac{\partial u}{\partial t}\left(1+\frac{\partial u}{\partial x}\right) + \frac{\partial v}{\partial t}\frac{\partial v}{\partial x}\right]\right\} dx \tag{12}$$

Summing Eq. (9) and Eq. (12) to have the total kinetic energy of the system and then considering the variations:

$$\begin{aligned}\delta\int_{t1}^{t2}(KE)dt = {} & \left(m_p + \sum_{j=1}^{n} M_j\right)\iint\left(\frac{\partial u}{\partial t}\delta\left(\frac{\partial u}{\partial t}\right) + \frac{\partial v}{\partial t}\delta\left(\frac{\partial v}{\partial t}\right)\right)dxdt \\ & + \sum_{j=1}^{n} M_j \iint\left(U_j{}^2\left[\delta\left(\frac{\partial u}{\partial x}\right) + \frac{\partial u}{\partial x}\delta\left(\frac{\partial u}{\partial x}\right)\right.\right. \\ & \left. - a\left(\delta\left(\frac{\partial u}{\partial x}\right) + \frac{\partial v}{\partial x}\delta\left(\frac{\partial v}{\partial x}\right)\right) + \frac{\partial v}{\partial x}\delta\left(\frac{\partial v}{\partial x}\right)\right] \\ & + 2U_j\left[\delta\left(\frac{\partial u}{\partial t}\right) + \frac{\partial u}{\partial t}\delta\left(\frac{\partial u}{\partial x}\right) + \frac{\partial u}{\partial x}\delta\left(\frac{\partial u}{\partial t}\right) + \frac{\partial v}{\partial t}\delta\left(\frac{\partial v}{\partial x}\right)\right. \\ & \left.\left. + \frac{\partial v}{\partial x}\delta\left(\frac{\partial v}{\partial t}\right)\right]\right)dxdt\end{aligned} \tag{13}$$

Integrating Eq. (13) and adopting the Lagrange notations for the variations in space and Newton notations for the variations in time, the terms varying in space and time are grouped as;

$$\delta\int_{t1}^{t2}(\mathrm{KE})\mathrm{dt}=\iint\left[-\left(\mathrm{m_p}+\sum_{j=1}^{n}\mathrm{M_j}\right)(\ddot{u}\delta u+\ddot{v}\delta v)-\sum_{j=1}^{n}\mathrm{M_j}{\mathrm{U_j}}^2(u''\delta u-av''\delta v+v''\delta v)-\sum_{j=1}^{n}\mathrm{M_j}\dot{\mathrm{U}}_j\delta u-\sum_{j=1}^{n}2\mathrm{M_j}\mathrm{U_j}\dot{u}'\delta u-\sum_{j=1}^{n}\mathrm{M_j}\dot{\mathrm{U}}_j u'\delta u-\sum_{j=1}^{n}2\mathrm{M_j}\mathrm{U_j}\dot{v}'\delta v-\sum_{j=1}^{n}\mathrm{M_j}\dot{\mathrm{U}}_j v'\delta v\right]\mathrm{dxdt}+\sum_{j=1}^{n}\mathrm{M_j}\mathrm{U_j}\int_{t1}^{t2}[\dot{u}_L\delta u+\dot{v}_L\delta v]\mathrm{dt} \tag{14}$$

2.1.2. Potential Energy

Semler et al [6] highlighted that the potential energy is as a result of the elastic deformation of the pipe and the effect of gravity. The deformation from elastic behavior of the pipe can be linked to the strain energy, which is expressed by Semler at al [6] as:

$$\mathcal{V}_\mathrm{p}=\frac{1}{2}\mathrm{EA}\int_0^\mathrm{L}\epsilon^2\mathrm{dx}+\frac{1}{2}\mathrm{EI}\int_0^\mathrm{L}(1+\epsilon)^2\mathrm{k}^2\mathrm{dx} \tag{15}$$

This is clearly the combinations of the axial strain effect and the bending strain effect where (E) denotes the Young's modulus, (I) denotes the pipe moment of inertia, (A) denotes the cross-sectional area, (ϵ) is the axial strain and (k) is the curvature term as expressed in Eq. (3).

The thermal effect can be introduced by considering the linear strain tensor as a sum of the strain contributions from the mechanical stress and the thermal effect. Semler et al [6] further decomposed the axial strain into a steady strain component due to externally applied tension ($\mathrm{T_0}$) and pressure force component ($\mathrm{P}=\mathrm{pA}$) and an oscillatory strain component due to the oscillations of the pipe. These can be expressed as:

$$\epsilon_\mathrm{ij}=\epsilon_\mathrm{ij}{}^{\sigma}+\epsilon_\mathrm{ij}{}^{\Delta}+\frac{\mathrm{T_0}-\mathrm{P}}{\mathrm{EA}} \tag{16}$$

While the stress contributing strain component can be obtained through the binomial expansion of Eq. (1) as:

$$\epsilon_\mathrm{ij}{}^{\sigma}=\frac{\partial\mathrm{u}}{\partial\mathrm{x}}-\frac{1}{2}\left(\frac{\partial\mathrm{u}}{\partial\mathrm{x}}\right)\left(\frac{\partial v}{\partial x}\right)^2+\frac{1}{2}\left(\frac{\partial v}{\partial x}\right)^2-\frac{1}{8}\left(\frac{\partial v}{\partial x}\right)^4 \tag{17}$$

Considering that the gradient of the transverse displacement of the pipe is far greater than the gradient of the longitudinal displacement $\left(\frac{\partial v}{\partial x}>\frac{\partial\mathrm{u}}{\partial\mathrm{x}}\right)$. Also, the thermal contributing strain component can be expressed in terms of the thermal expansively (α) and the difference in temperatures (ΔT) as:

$$\epsilon_{ij}{}^{\Delta}=(-\alpha\Delta T) \tag{18}$$

Substituting Eq. (17) and Eq. (18) into Eq. (16) and then substituting Eq. (16), Eq. (3) and Eq. (5) in to Eq. (15) resulting to:

$$\mathcal{V}_p = \frac{1}{2}EA\int_0^L \left[\left(u' - \frac{1}{2}u'v'^2 + \frac{1}{2}v'^2 - \frac{1}{8}v'^4\right) + \frac{T_0 - P}{EA} + (-\alpha\Delta T)\right]^2 dx + \frac{1}{2}EI\int_0^L \left[v''^2 - 2v''^2u' - 2v''^2u''^2 - 2v'v''u''\right]dx \tag{19}$$

With the reference plane in the same direction as the gravitational acceleration, the effect of gravity can be expressed as:

$$\mathcal{V}_g = g\left(\sum_{j=1}^{n} M_j + m\right)\int_0^L (x+u)dx \tag{20}$$

Combining equations (19) and (20), the potential energy of the system is expressed as:

$$\begin{aligned}\delta\int_{t1}^{t2}(PE)dt = EA\iint &\left[\left(\frac{T_0 - P}{EA} - (\alpha\Delta T)\right)\left(\delta u' - u'v'\delta v' - \frac{1}{2}v'^2\delta u' + v'\delta v' - \frac{1}{2}v'^3\delta v'\right)\right.\\ &+ \left(u' - \frac{1}{2}u'v'^2 + \frac{1}{2}v'^2 - \frac{1}{8}v'^4\right)\left(\delta u' - u'v'\delta v' - \frac{1}{2}v'^2\delta u' + v'\delta v' - \frac{1}{2}v'^3\delta v'\right)\Big]dxdt\\ &+ EI\iint\left[v''\delta v'' - v''\delta u' - 2u'v''\delta v'' - 2v''^2v'\delta v' - 2v'^2v''\delta v'' - v'v''\delta u'' - v'u''\delta v'' - v''u''\delta v'\right]dxdt\\ &+ g\left(\sum_{j=1}^{n} M_j + m\right)\int_0^L(\delta u)dxdt\end{aligned} \tag{21}$$

According to Semler at al [6], for a pipe of length L=1, with $|u|\sim 0.01, and\ |v|\sim 0.1$, neglecting terms of the order 0.0001 and below.

Integrating Eq. (21) and collecting terms that varies in time and space as:

$$\begin{aligned}\delta\int_{t1}^{t2}(PE)dt = \iint &(-EAu''\delta u - EA(u'v'' + v'u'')\delta v\\ &- EA\left(\frac{3}{2}v'^2v''\right)\delta v\\ &+ (T_0 - P - EA(\alpha\Delta T))(u'v'' + v'u'')\delta v\\ &+ (T_0 - P - EA(\alpha\Delta T))\left(\frac{3}{2}v'^2v''\right)\delta v - EAv'v''\delta u\\ &+ (T_0 - P - EA(\alpha\Delta T))v''\delta v\\ &+ (T_0 - P - EA(\alpha\Delta T))v'v''\delta u + EIv''''\delta v\\ &- EI(v''''v' + v''v''')\delta u\\ &- EI\left(3u'''v'' + 4v'''u'' + 2u'v'''' + 2v'^2v'''' + 8v'v''v''' + 2v''^3\right)\delta v - (T_0 - P - EA(\alpha\Delta T))'\delta u\\ &+ \left(m + \sum_{j=1}^{n} M_j\right)g\delta u)dxdt\end{aligned} \tag{22}$$

2.1.3. Non-Conservative Work Done

As illustrated by Sinir [13], the damping effect can be accounted for by taking the first variations of the non-conservative force:

$$\int_{t1}^{t2} \delta W_{nc} = \int_{t1}^{t2} c\dot{v}\delta v dt \tag{23}$$

where c is the coefficient of viscous damping. Also, the right hand side term of the Hamilton's equation (6):

$$\text{rhs} = \sum_{j=1}^{n} M_j U_j \int_{t1}^{t2} \left[\left(\dot{u}_L + \sum_{j=1}^{n} U_j u'_L \right) \delta u + \left(\dot{v}_L + \sum_{j=1}^{n} U_j v'_L \right) \delta v \right] dt = 0 \tag{24}$$

$$= \sum_{j=1}^{n} M_j U_j \int_{t1}^{t2} (\dot{u}_L \delta u + \dot{v}_L \delta v) dt + \sum_{j=1}^{n} M_j U^2{}_j \int_{t1}^{t2} \left(u'_L \delta u + v'_L \delta v \right) dt \tag{25}$$

The first term of equation (25) is identical to the last term of equation (14), therefore the rhs becomes:

$$\sum_{j=1}^{n} M_j U^2{}_j \int_{t1}^{t2} \left(u'_L \delta u + v'_L \delta v \right) dt \tag{26}$$

Physically, this implies a non-classical boundary condition at the free end for a discharging cantilever pipe:

$$EIv'''_L = \sum_{j=1}^{n} M_j U^2{}_j \int_{t1}^{t2} v'_L \delta v dt \tag{27}$$

Thus, a force is imposed at the free end if the velocity of the exiting fluid is not tangential to the pipe. However this study assumes that the exiting flow remains tangential to the pipe at the free end, therefore classical boundary condition holds at the free end.

2.2. Equation of Motion for Multiphase Flow

Summing equations (14), (22), (23) and (25), the system's equation of motion can be expressed as:

$$\begin{aligned} \left(m + \sum_{j=1}^{n} M_j \right) \ddot{u} + \sum_{j=1}^{n} M_j \dot{U}_j + \sum_{j=1}^{n} 2 M_j U_j \dot{u}' + \sum_{j=1}^{n} M_j U_j{}^2 u'' + \sum_{j=1}^{n} M_j \dot{U}_j u' \\ - EAu'' - EI\left(v'''' v' + v'' v''' \right) \\ + (T_0 - P - EA(\alpha \Delta T) - EA) v' v'' \\ - \left(T_0 - P - EA(\alpha \Delta T) \right)' + \left(m + \sum_{j=1}^{n} M_j \right) g = 0 \end{aligned} \tag{28}$$

$$\left(m+\sum_{j=1}^{n}M_j\right)\ddot{v}+\sum_{j=1}^{n}2M_jU_j\dot{v}'+\sum_{j=1}^{n}M_j\,{U_j}^2v''-\sum_{j=1}^{n}aM_j\,{U_j}^2v''+\sum_{j=1}^{n}M_j\dot{U}_jv' + EIv'''' - \left(T_0-P-EA(\alpha\Delta T)\right)v'' + C\dot{v} - EI\left(3u'''v''+4v'''u''+2u'v''''+2{v'}^2v''''+8v'v''v'''+2{v''}^3\right) + (T_0-P-EA(\alpha\Delta T)-EA)\left(u'v''+v'u''+\frac{3}{2}{v'}^2v''\right)=0 \tag{29}$$

The associated boundary conditions are:

$$v(0)=v'(0)\ and\ v''(L)=v'''(L)=0 \tag{30}$$

$$u(0)=u'(L)=0 \tag{31}$$

Where the terms represent:

The inertia force terms: $\left(m+\sum_{j=1}^{n}M_j\right)\ddot{u}\ and\ \left(m+\sum_{j=1}^{n}M_j\right)\ddot{v}$

The Coriolis force: $\sum_{j=1}^{n}2M_jU_j\dot{u}'\ \ and\ \sum_{j=1}^{n}2M_jU_j\dot{v}'$

The centrifugal force: $\sum_{j=1}^{n}M_j\,{U_j}^2u''\ and\ a\sum_{j=1}^{n}M_j\,{U_j}^2v''$

The forces due to gravity:$\left(m+\sum_{j=1}^{n}M_j\right)g$

The bending stiffness term: EIv''''

The axial stiffness term: EAu''

The damping term: $C\dot{v}$

The forces due to unsteady flow: $\sum_{j=1}^{n}M_j\dot{U}_j$

The gradient terms: $\left(T_0-P-EA(\alpha\Delta T)\right)'$

Equations (28), (29), (30) and (31) are the governing equations and boundary conditions for a tensioned cantilever pipe conveying pressurized unsteady multiphase flow under thermal loading.

2.2.1. Dimensionless Equation of Motion for Multiphase Flow

The equation of motion may be rendered dimensionless to make the analysis of the system more robust and not constraint to one specific system by introducing the following non-dimensional quantities;

$$\bar{u}=\frac{u}{L}\ ,\quad \bar{v}=\frac{v}{L}\ ,\quad \bar{t}=\left[\frac{EI}{\sum M_j+m}\right]^{1/2}\frac{t}{L^2}\ ,\quad \bar{U}_j=\left[\frac{M_j}{EI}\right]^{1/2}UL\ , \qquad \gamma=\frac{\sum M_j+m}{EI}L^3g, \tag{32}$$

$$\beta_j=\frac{M_j}{\sum M_j+m},\quad \Psi_j=\frac{M_j}{\sum M_j},\ Damping\ term:\mu=\frac{CL^2}{\sqrt{\sum(M_j+m)EI}}$$

$$Tension:\Pi_0=\frac{T_oL^2}{EI}\ ,Flexibility:\Pi_1=\frac{EAL^2}{EI},\qquad Presure:\Pi_2=\frac{PL^2}{EI}$$

$$\ddot{\bar{u}} + \sum_{j=1}^{n} \dot{\bar{U}}_j \sqrt{\Psi_j}\sqrt{\beta_j} + 2\sum_{j=1}^{n} \bar{U}_j \sqrt{\Psi_j}\sqrt{\beta_j}\dot{\bar{u}}' + \sum_{j=1}^{n} \Psi_j \bar{U}_j^{\,2}\bar{u}'' + \sum_{j=1}^{n} \dot{\bar{U}}_j \sqrt{\Psi_j}\sqrt{\beta_j}\bar{u}' - \Pi_1\bar{u}'' - \left(\bar{v}''''\bar{v}' + \bar{v}''\bar{v}'''\right) + (\Pi_0 - \Pi_2 - \Pi_1(\alpha\Delta T) - \Pi_1)\bar{v}'\bar{v}'' - \left(\Pi_0 - \Pi_2 - \Pi_1(\alpha\Delta T)\right)' + \gamma = 0$$

$$\ddot{\bar{v}} + 2\sum_{j=1}^{n} \bar{U}_j \sqrt{\Psi_j}\sqrt{\beta_j}\dot{\bar{v}}' + \sum_{j=1}^{n} \Psi_j \bar{U}_j^{\,2}\bar{v}'' - a\sum_{j=1}^{n} \Psi_j \bar{U}_j^{\,2}\bar{v}'' + \sum_{j=1}^{n} \dot{\bar{U}}_j \sqrt{\Psi_j}\sqrt{\beta_j}\bar{v}' - \left(\Pi_0 - \Pi_2 - \Pi_1(\alpha\Delta T)\right)v'' + \bar{v}'''' + \mu\dot{v} - \left(3\bar{u}''''\bar{v}'' + 4\bar{v}'''\bar{u}'' + 2\bar{u}'\bar{v}'''' + 2\bar{v}'^{2}\bar{v}'''' + 8\bar{v}'\bar{v}''\bar{v}''' + 2\bar{v}''^{3}\right) + (\Pi_0 - \Pi_2 - \Pi_1(\alpha\Delta T) - \Pi_1)\left(\bar{u}'\bar{v}'' + \bar{v}'\bar{u}'' + \frac{3}{2}\bar{v}'^{2}\bar{v}''\right) = 0 \tag{33}$$

The dimensionless boundary conditions are:

$$\bar{v}(0) = \bar{v}'(0) \; and \; \bar{v}''(L) = \bar{v}'''(L) = 0 \tag{34}$$

$$\bar{u}(0) = \bar{u}'(L) = 0 \tag{35}$$

In these equations, $\bar{u}$ *and* $\bar{v}$ are respectively, the dimensionless displacements in the longitudinal and transverse direction, $(\bar{U}_j)$ is the flow velocities of the constituent phases/components used in the parametric studies of the dynamics of the system, (β_j) is the mass ratio same as in single phase flows as derived by Semler et al [6] and Paidoussis [20], (Ψ_j) is another mass ratio which is unique to multiphase flow relating the fluid mass independent of the mass of the pipe, (γ) is the gravity term, (μ) is the damping term and (Π_0, Π_1, Π_2) represent the Tension term, Flexibility term and the pressurization term respectively.

2.2.2. Dimensionless Equation of Motion for Two Phase Flow

The governing equation can be reduced to that of a two phase as:

$$\ddot{\bar{u}} + \dot{\bar{U}}_1\sqrt{\Psi_1}\sqrt{\beta_1} + \dot{\bar{U}}_2\sqrt{\Psi_2}\sqrt{\beta_2} + 2\bar{U}_1\sqrt{\Psi_1}\sqrt{\beta_1}\dot{\bar{u}}' + 2\bar{U}_2\sqrt{\Psi_2}\sqrt{\beta_2}\dot{\bar{u}}' + \Psi_1\bar{U}_1^{\,2}\bar{u}'' + \Psi_2\bar{U}_2^{\,2}\bar{u}'' + \dot{\bar{U}}_1\sqrt{\Psi_1}\sqrt{\beta_1}\bar{u}' + \dot{\bar{U}}_2\sqrt{\Psi_2}\sqrt{\beta_2}\bar{u}' - \Pi_1\bar{u}'' - \left(\bar{v}''''\bar{v}' + \bar{v}''\bar{v}'''\right) + (\Pi_0 - \Pi_2 - \Pi_1(\alpha\Delta T) - \Pi_1)\bar{v}'\bar{v}'' - \left(\Pi_0 - \Pi_2 - \Pi_1(\alpha\Delta T)\right)' + \gamma = 0 \tag{36}$$

$$\ddot{\bar{v}} + 2\bar{U}_1\sqrt{\Psi_1}\sqrt{\beta_1}\dot{\bar{v}}' + 2\bar{U}_2\sqrt{\Psi_2}\sqrt{\beta_2}\dot{\bar{v}}' + \Psi_1\bar{U}_1^{\,2}\bar{v}'' + \Psi_2\bar{U}_2^{\,2}\bar{v}'' - a\Psi_1\bar{U}_1^{\,2}\bar{v}'' - a\Psi_2\bar{U}_2^{\,2}\bar{v}'' + \mu\dot{v} + \dot{\bar{U}}_1\sqrt{\Psi_1}\sqrt{\beta_1}\bar{v}' + \dot{\bar{U}}_2\sqrt{\Psi_2}\sqrt{\beta_2}\bar{v}' - \left(\Pi_0 - \Pi_2 - \Pi_1(\alpha\Delta T)\right)v'' + \bar{v}'''' - \left(3\bar{u}''''\bar{v}'' + 4\bar{v}'''\bar{u}'' + 2\bar{u}'\bar{v}'''' + 2\bar{v}'^{2}\bar{v}'''' + 8\bar{v}'\bar{v}''\bar{v}''' + 2\bar{v}''^{3}\right) + (\Pi_0 - \Pi_2 - \Pi_1(\alpha\Delta T) - \Pi_2)\left(\bar{u}'\bar{v}'' + \bar{v}'\bar{u}'' + \frac{3}{2}\bar{v}'^{2}\bar{v}''\right) = 0 \tag{37}$$

The associated boundary conditions are:

$$\bar{v}(0) = \bar{v}'(0) \; and \; \bar{v}''(L) = \bar{v}'''(L) = 0 \tag{38}$$

$$\bar{u}(0) = \bar{u}'(L) = 0 \tag{39}$$

2.2.3. Governing Equation for a steady two phase flow

$$\ddot{\bar{u}} + \bar{U}_1 C21\dot{\bar{u}}' + \bar{U}_2 C22\dot{\bar{u}}' + C31\overline{U_1}^2\bar{u}'' + C32\overline{U_2}^2\bar{u}'' - C5\bar{u}'' - \left(\bar{v}''''\bar{v}' + \bar{v}''\bar{v}'''\right) + C6\bar{v}'\bar{v}'' - C7' + \gamma = 0 \tag{40}$$

$$\ddot{\bar{v}} + \bar{U}_1 C21\dot{\bar{v}}' + \bar{U}_2 C22\dot{\bar{v}}' + C31\overline{U_1}^2\bar{v}'' + C32\overline{U_2}^2\bar{v}'' - aC31\overline{U_1}^2\bar{v}'' - aC32\overline{U_2}^2\bar{v}'' + Cm\dot{v} - C7v'' + \bar{v}'''' - \left(3\bar{u}'''\bar{v}'' + 4\bar{v}'''\bar{u}'' + 2\bar{u}'\bar{v}'''' + 2\bar{v}'^2\bar{v}'''' + 8\bar{v}'\bar{v}''\bar{v}''' + 2\bar{v}''^3\right) + C6\left(\bar{u}'\bar{v}'' + \bar{v}'\bar{u}'' + \frac{3}{2}\bar{v}'^2\bar{v}''\right) = 0 \tag{41}$$

For a steady flow, velocities are not changing with time, therefore;

$$\dot{\overline{U_1}} = \dot{\overline{U_2}} = 0 \tag{42}$$

The associated boundary conditions are:

$$\bar{v}(0) = \bar{v}'(0) \; and \; \bar{v}''(L) = \bar{v}'''(L) = 0 \tag{43}$$

$$\bar{u}(0) = \bar{u}'(L) = 0 \tag{44}$$

Equations (40) to (44) are obtained using the notations:

$C21 = 2\sqrt{\Psi_1}\sqrt{\beta_1}$

$C22 = 2\sqrt{\Psi_2}\sqrt{\beta_2}$

$C31 = \Psi_1$

$C32 = \Psi_2$

$C41 = C11$

$C42 = C12$

$C5 = \Pi_1$

$C6 = \Pi_0 - \Pi_2 - \Pi_1(\alpha\Delta T) - \Pi_1$

$C7 = \Pi_0 - \Pi_2 - \Pi_1(\alpha\Delta T)$

$Cm = \mu$

2.3. Empirical Gas–Liquid Two-Phase Flow Model

The components velocities in terms of the superficial velocities are expressed as:

$$V_g = U_g vf, \quad V_l = U_l(1 - vf) \tag{45}$$

Where U_g and U_l are the superficial flow velocities. Adopting the Chisholm empirical relations Woldesemayat and Ghajar [14], Void fraction:

$$vf = \left[1 + \sqrt{1 - \mathrm{x}\left(1 - \frac{\rho_l}{\rho_g}\right)}\left(\frac{1-\mathrm{x}}{\mathrm{x}}\right)\left(\frac{\rho_g}{\rho_l}\right)\right]^{-1} \tag{46}$$

Slip Ratio:

$$S = \frac{V_g}{V_l} = \left[1 - \mathrm{x}\left(1 - \frac{\rho_l}{\rho_g}\right)\right]^{1/2} \tag{47}$$

The vapour quality: (x) The densities of the liquid and gas phases respectively: (ρ_l and ρ_g)
Mixture Velocity:

$$V_T = U_g vf + U_l(1 - vf) \tag{48}$$

Individual Velocities:

$$V_l = \frac{V_T}{S+1}, V_g = \frac{SV_T}{S+1} \tag{49}$$

For various void fractions (0.1, 0.3, 0.5, 0.7 and 0.9) and a series of mixture velocities, the corresponding slip ratio and individual velocities are estimated and used for numerical calculations.

Single phase flow velocity can be recovered by making the slip ratio to be zero.

3. Method of Solution

Exact solutions of nonlinear equations are almost not available; an approximate solution will be sought for by utilizing the multiple time scale perturbation technique. This approach is applied directly to the partial differential equations (40) and (41), given that the common method of discretizing the equations first and then applying perturbation method yields less accurate results for finite mode truncations and higher order perturbation schemes [15-18].

Adopting perturbation techniques, it is necessary to decide the terms to be considered small or weak. However, the study considers the contributions of the nonlinear terms, damping term, gradient term and gravity term to be small compared to the linear terms.

The damping coefficient is ordered so that the effect of damping and nonlinearity appear in the same perturbation equation.

$$\begin{aligned} \ddot{\bar{u}} + \bar{U}_1 C21\dot{\bar{u}}' + \bar{U}_2 C22\dot{\bar{u}}' + C31\overline{U_1}^2\bar{u}'' + C32\overline{U_2}^2\bar{u}'' - C5\bar{u}'' \\ + \varepsilon\left(-\left(\bar{v}''''\bar{v}' + \bar{v}''\bar{v}'''\right) + C6\bar{v}'\bar{v}'' - C7' + \gamma\right) = 0 \end{aligned} \tag{50}$$

$$\begin{aligned} \ddot{\bar{v}} + \bar{U}_1 C21\dot{\bar{v}}' + \bar{U}_2 C22\dot{\bar{v}}' + C31\overline{U_1}^2\bar{v}'' + C32\overline{U_2}^2\bar{v}'' - aC31\overline{U_1}^2\bar{v}'' \\ - aC32\overline{U_2}^2\bar{v}'' + \varepsilon Cm\dot{v} - C7v'' + \bar{v}'''' \\ + \varepsilon\left(-\left(3\bar{u}'''\bar{v}'' + 4\bar{v}'''\bar{u}'' + 2\bar{u}'\bar{v}'''' + 2\bar{v}'^2\bar{v}'''' \right.\right. \\ \left.\left. + 8\bar{v}'\bar{v}''\bar{v}''' + 2\bar{v}''^3\right) + C6\left(\bar{u}'\bar{v}'' + \bar{v}'\bar{u}'' + \frac{3}{2}\bar{v}'^2\bar{v}''\right)\right) \\ = 0 \end{aligned} \tag{51}$$

We seek an approximate solution for $\bar{u}$ *and* $\bar{v}$ of the form:

$$\bar{u} = \bar{u}_0(T_0, T_1) + \varepsilon\bar{u}_1(T_0, T_1) + \varepsilon^2\bar{u}_2(T_0, T_1) + \cdots \quad (52)$$

$$\bar{v} = \bar{v}_0(T_0, T_1) + \varepsilon\bar{v}_1(T_0, T_1) + \varepsilon^2\bar{v}_2(T_0, T_1) + \cdots \quad (53)$$

Two time scales are needed $T_0 = t$ and $T_1 = \varepsilon t$

Where ε is a small dimensionless measure of the amplitude of $\bar{u}$ and $\bar{v}$, used as a book-keeping parameter. Then, the time derivatives are:

$$\frac{d}{dt} = D_0 + \varepsilon D_1 + \varepsilon^2 D_2 + \ldots \quad (54)$$

$$\frac{d^2}{dt^2} = {D_0}^2 + 2\varepsilon D_0 D_1 + \varepsilon^2({D_1}^2 + 2D_0 D_2) + \ldots \quad (55)$$

$Where\ D_n = \frac{\partial}{\partial T_n}$

Substituting Eq. (55), Eq. (54), Eq. (53) and Eq. (52) into Eq. (50) and Eq. (51) and equating the coefficients of (ε) to zero and are respectively:

U-Equation:

$$O(\varepsilon^0). \quad {D_0}^2\bar{u}_0 + C21D_0{\bar{u}_0}'\bar{U}_1 + C22D_0{\bar{u}_0}''\bar{U}_2 + C31{\bar{u}_0}''{\bar{U}_1}^2 + C32{\bar{u}_0}''{\bar{U}_2}^2 - C5{\bar{u}_0}'' = 0 \quad (56)$$

$$O(\varepsilon^1). \quad {D_0}^2\bar{u}_1 + C21D_0{\bar{u}_1}'\bar{U}_1 + C22D_0{\bar{u}_1}'\bar{U}_2 + 2D_1D_0\bar{u}_0 + C31{\bar{u}_1}''{\bar{U}_1}^2 + C32{\bar{u}_1}''{\bar{U}_2}^2 + C21D_0{\bar{u}_0}'\bar{U}_1 + C22D_0{\bar{u}_0}'\bar{U}_2 - C5{\bar{u}_1}'' - {\bar{v}_0}''''{\bar{v}_0}' - C7' - \gamma - {\bar{v}_0}''{\bar{v}_0}''' + C6{\bar{v}_0}'{\bar{v}_0}'' = 0 \quad (57)$$

V-Equation:

$$O(\varepsilon^0). \quad {D_0}^2\bar{v}_0 - C7{\bar{v}_0}' + {\bar{v}_0}'''' + C21D_0{\bar{v}_0}'\bar{U}_1 + C22D_0{\bar{v}_0}'\bar{U}_2 + C31{\bar{v}_0}''{\bar{U}_1}^2 + C32{\bar{v}_0}''{\bar{U}_2}^2 - aC31{\bar{v}_0}''{\bar{U}_1}^2 - aC32{\bar{v}_0}''{\bar{U}_2}^2 = 0 \quad (58)$$

$$O(\varepsilon^1). \quad {D_0}^2\bar{v}_1 - C7{\bar{v}_1}'' + {\bar{v}_1}'''' + 2{\bar{u}_0}'{\bar{v}_0}'''' + 4{\bar{u}_0}''{\bar{v}_0}''' + 3{\bar{v}_0}''{\bar{v}_0}''' + 2{\bar{v}_0}^{3''} + 2D_0D_1\bar{v}_0 + C31{\bar{v}_1}''{\bar{U}_1}^2 + C32{\bar{v}_1}''{\bar{U}_2}^2 + 8{\bar{v}_0}'{\bar{v}_0}''{\bar{v}_0}''' + C6{\bar{u}_0}'{\bar{v}_0}'' + C6{\bar{u}_0}''{\bar{v}_0}' + CmD_0\bar{v}_0 + \frac{3}{2}C6{\bar{v}_0}^{2'}{\bar{v}_0}'' + C21D_0{\bar{v}_0}'\bar{U}_1 + C22D_0{\bar{v}_0}'\bar{U}_2 + C21D_1{\bar{v}_0}'\bar{U}_1 + C22D_1{\bar{v}_0}'\bar{U}_2 - aC31{\bar{v}_1}''{\bar{U}_1}^2 - aC32{\bar{v}_1}''{\bar{U}_2}^2 = 0 \quad (59)$$

The order zero problems for both the axial and transverse vibration of the cantilever pipe have the form of an undamped and unforced flow induced vibration problem. This will be used to estimate the linear natural frequencies and mode shapes.

3.1. Natural Frequencies and Modal Functions

Estimation of the Natural frequencies and modal function is an order zero problem that can be determined by resolving Eq. (56) and Eq. (58).

The homogeneous solution of the leading order equations Eq. (56) and Eq. (58) can be expressed as:

$$\bar{u}(x,T_0,T_1)_0 = \phi(x)_n\, exp(i\omega_n T_0) + CC \tag{60}$$

$$\bar{v}(x,T_0,T_1)_0 = \eta(x)_n\, exp(i\lambda_n T_0) + CC \tag{61}$$

Where (CC) is the complex conjugate, $\phi(x)_n$ *and* $\eta(x)_n$ are the modal functions for the axial and transverse vibrations for each mode (n) and ω_n *and* λ_n are the eigenvalues for the axial and transverse vibrations for each mode (n).The eigenvalues are complex values with complex conjugate pair of solutions. Substituting Eq. (60) and Eq. (61) into Eq. (56) and Eq. (58) results to:

$$\left(C31\bar{U}_1{}^2 + C32\bar{U}_2{}^2 - C5\right)\phi(x)_n{}'' + (C21\bar{U}_1 + C22\bar{U}_2)i\omega_n\phi(x)_n{}' - \phi(x)_n\omega_n{}^2 = 0 \tag{62}$$

$$\eta(x)_n{}'''' + \left(C31\bar{U}_1{}^2 + C32\bar{U}_2{}^2 - C7 - aC31\bar{U}_1{}^2 - aC32\bar{U}_2{}^2\right)\eta(x)_n{}'' + (C21\bar{U}_1 + C22\bar{U}_2)i\lambda_n\eta(x)_n{}' - \eta(x)_n\lambda_n{}^2 = 0 \tag{63}$$

The general solution to the ordinary differential equations Eq. (62) and Eq. (63) are expressed as:

$$\phi(x)_n = G1_n\, exp(ik_1x) + G2_n\, exp(ik_2x) \tag{64}$$

$$\eta(x)_n = H1(exp(iz_1x) + H2exp(iz_2x) + H3\, exp(iz_3x) + H4ex\, p(iz_4x) \tag{65}$$

3.1.1. Solution to axial vibration problem

Substituting Eq. (64) into Eq. (62) gives a quadratic relation of the form:

$$\left(C5 - C31\bar{U}_1{}^2 - C32\bar{U}_2{}^2\right)k^2 - (C21\bar{U}_1 + C22\bar{U}_2)i\omega_n k - \omega_n{}^2 = 0 \tag{66}$$

Solving the quadratic equation (66) for the wave numbers (k) as a function of the eigenvalue (ω_n):

$$k_1 = \omega_n\left[\frac{\frac{C21\bar{U}_1}{2} + \frac{C22\bar{U}_2}{2} + \frac{\sqrt{C21^2\bar{U}_1{}^2 + 2C21C22\bar{U}_1\bar{U}_2 + C22^2\bar{U}_2{}^2 - 4C31\bar{U}_1{}^2 - 4C32\bar{U}_2{}^2 + 4C5}}{2}}{C5 - C31\bar{U}_1{}^2 - C32\bar{U}_2{}^2}\right] \tag{67}$$

$$k_2 = \omega_n\left[\frac{\frac{C21\bar{U}_1}{2} + \frac{C22\bar{U}_2}{2} - \frac{\sqrt{C21^2\bar{U}_1{}^2 + 2C21C22\bar{U}_1\bar{U}_2 + C22^2\bar{U}_2{}^2 - 4C31\bar{U}_1{}^2 - 4C32\bar{U}_2{}^2 + 4C5}}{2}}{C5 - C31\bar{U}_1{}^2 - C32\bar{U}_2{}^2}\right] \tag{68}$$

In order to obtain the eigenvalue, Eq. (64) is substituted into the boundary conditions in Eq. (44):

$$\frac{\partial\phi(l,t)}{\partial x} = 0 \; and \; \phi(0,t) = 0 \tag{69}$$

$$G1 + G2 = 0 \tag{70}$$

$$G1k_1 i\, exp(iLk_1) + G2k_2 i\, exp(iLk_2) = 0 \tag{71}$$

In matrix form:

$$\underbrace{\begin{pmatrix} 1 & 1 \\ ik_1 exp(iLk_1) & ik_2 exp(iLk_2) \end{pmatrix}}_{D} \begin{pmatrix} G1 \\ G2 \end{pmatrix} = 0 \tag{72}$$

For a non-trivial solution, the determinant of (D) must varnish;

$$-ik_1\, exp(iLk_1) + ik_2\, exp(iLk_2) = 0 \tag{73}$$

Substituting Eq. (67) and Eq. (68) into Eq. (73) and solving for the eigenvalue:

$$\omega_n = \frac{2\pi n - i.ln\left(\frac{b}{a}\right)}{(a-b)L}, \qquad n = 1,2,3,\ldots \tag{74}$$

$$a = \frac{\frac{C21\bar{U}_1}{2} + \frac{C22\bar{U}_2}{2} + \frac{\sqrt{C21^2\bar{U}_1{}^2 + 2C21C22\bar{U}_1\bar{U}_2 + C22^2\bar{U}_2{}^2 - 4C31\bar{U}_1{}^2 - 4C32\bar{U}_2{}^2 + 4C5}}{2}}{C5 - C31\bar{U}_1{}^2 - C32\bar{U}_2{}^2}$$

$$b = \frac{\frac{C21\bar{U}_1}{2} + \frac{C22\bar{U}_2}{2} - \frac{\sqrt{C21^2\bar{U}_1{}^2 + 2C21C22\bar{U}_1\bar{U}_2 + C22^2\bar{U}_2{}^2 - 4C31\bar{U}_1{}^2 - 4C32\bar{U}_2{}^2 + 4C5}}{2}}{C5 - C31\bar{U}_1{}^2 - C32\bar{U}_2{}^2}$$

Eq. (74) is the pipe's axial vibration eigenvalue. Solving Eq. (70) and Eq. (71) gives the constants G1 and G2. Therefore, the modal function for the axial vibration of the pipe is expressed as:

$$\phi(x)_n = G1_n\, exp(ik_1 x) + G2_n\, exp(ik_2 x) \tag{75}$$

Substituting Eq. (64) into Eq. (60) yields:

$$\begin{aligned} \bar{u}(x,T_0)_0 &= \sum_{j=1}^{2} G_{jn}\, exp\left(ik_{jn}x\right) exp(i\omega_n T_0) \\ &= \sum_{j=1}^{2} G_{jn}\, exp\left(-Im\left(k_{jn}x\right) - Im(\omega_n T_0)\right) exp\big(i(\mathrm{Re}\left(k_{jn}x\right) \\ &\quad + Re(\omega_n T_0))\big) \end{aligned} \tag{76}$$

It is clear from Eq. (76) that the real part is the natural frequency and the imaginary part is the amplitude. However, a marginally negative value of the imaginary part of any of the eigenvalue (ω_n) will cause the axial displacement ($\bar{u}$) to grow exponentially in time and this signifies the onset of the system's instability.

3.1.2. Solution to Transverse Vibration Problem

Substituting Eq. (65) into Eq. (63) gives a quartic relation:

$$z^4{}_{jn} + \left(C7 - C31\bar{U}_1{}^2 - C32\bar{U}_2{}^2 + aC31\bar{U}_1{}^2 + aC32\bar{U}_2{}^2\right) z^2{}_{jn} - (C21\bar{U}_1 + C22\bar{U}_2) z_{jn}\lambda_n - \lambda^2{}_n = 0 \tag{77}$$

$j = 1,2,3,4\ and\ n = 1,2,3,4,5 \ldots$

In order to obtain the eigenvalue, Eq. (65) is substituted into the boundary conditions in Eq. (43):

$$\eta(0) = \eta'(0)\ and\ \eta''(L) = \eta'''(L) = 0 \tag{78}$$

This gives four algebraic equations which can be expressed in matrix form as:

$$\underbrace{\begin{bmatrix} 1 & 1 & 1 & 1 \\ z_{1n} & z_{2n} & z_{3n} & z_{4n} \\ (z_{1n})^2.\exp(i.z_{1n}) & (z_{2n})^2.\exp(i.z_{2n}) & (z_{3n})^2.\exp(i.z_{3n}) & (z_{4n})^2.\exp(i.z_{4n}) \\ (z_{1n})^3.\exp(i.z_{1n}) & (z_{2n})^3.\exp(i.z_{2n}) & (z_{3n})^3.\exp(i.z_{3n}) & (z_{4n})^3.\exp(i.z_{4n}) \end{bmatrix}}_{G} \cdot \begin{bmatrix} 1 \\ H2_n \\ H3_n \\ H4_n \end{bmatrix} . H1_n = \begin{pmatrix} 0 \\ 0 \\ 0 \\ 0 \end{pmatrix}$$

For a non-trivial solution, the determinant of (G) must varnish, That is:

$$DET(G) = 0 \tag{79}$$

In order to find modal solutions of (λ), Eq. (77) and Eq. (79) must be solve simultaneously, this can be solved numerically using nonlinear numerical routine.

The mode function of the transverse vibration corresponding to the nth eigenvalue is expressed as:

$$\eta(x)_n = H1_n.[e^{x.z_{1n}.i} - (A + B + C + D) - E] \tag{80}$$

$$A = \frac{e^{x.z_{4n}.i}.\ [e^{z_{1n}.i}.(z_{1n})^3.z_{2n} - e^{z_{1n}.i}.(z_{1n})^3.\ z_{3n} - e^{z_{1n}.i}.\ z_{4n}.(z_{1n})^2.z_{2n}}{(z_{2n} - z_{4n}).(z_{3n} - z_{4n}).[e^{z_{2n}.i}.(z_{2n})^2 - e^{z_{3n}.i}.(z_{3n})^2]}$$

$$B = \frac{e^{x.z_{4n}.i}.\ [e^{z_{1n}.i}.z_{4n}.(z_{1n})^2.z_{3n} - e^{z_{2n}.i}.z_{1n}.(z_{2n})^3 + e^{z_{2n}.i}.\ z_{4n}.\ z_{1n}.(z_{2n})^2}{(z_{2n} - z_{4n}).(z_{3n} - z_{4n}).[e^{z_{2n}.i}.(z_{2n})^2 - e^{z_{3n}.i}.(z_{3n})^2]}$$

$$C = \frac{e^{x.z_{4n}.i}.\ [e^{z_3.i}.z_{1n}.(z_{3n})^3 - e^{z_3.i}.z_{4n}.z_{1n}.(z_{3n})^2 + e^{z_{2n}.i}.(z_{2n})^3.z_{3n}}{(z_{2n} - z_{4n}).(z_{3n} - z_{4n}).[e^{z_{2n}.i}.(z_{2n})^2 - e^{z_{3n}.i}.(z_{3n})^2]}$$

$$D = \frac{e^{x.z_{4n}.i}.\ [-e^{z_{2n}.i}.z_{4n}.(z_{2n})^2.z_{3n} - e^{z_3.i}.z_{2n}.(z_{3n})^3 + e^{z_3.i}.z_{4n}.z_{2n}.(z_{3n})^2}{(z_{2n} - z_{4n}).(z_{3n} - z_{4n}).[e^{z_{2n}.i}.(z_{2n})^2 - e^{z_{3n}.i}.(z_{3n})^2]}$$

$$E = \frac{e^{x.z_{2n}.i}.(z_{1n} - z_{4n}).[e^{z_1.i}.\ (z_{1n})^2 - e^{z_3.i}.(z_{3n})^2]}{(z_{2n} - z_{4n}).\ [e^{z_2.i}.(z_{2n})^2 - e^{z_3.i}.(z_{3n})^2]} + \frac{e^{x.z_3.i}.(z_{1n} - z_{4n}).[e^{z_{1n}.i}.\ (z_{1n})^2 - e^{z_2 i}.(z_{2n})^2]}{(z_{3n} - z_{4n}).\ [e^{z_2.i}.(z_{2n})^2 - e^{z_3.i}.(z_{3n})^2]}$$

Substituting Eq. (65) into Eq. (61) yields:

$$\bar{v}(x,T_0)_0 = \sum_{j=1}^{4} H_{jn}\, exp\left(iz_{jn}x\right) exp(i\lambda_n T_0) \tag{81}$$
$$= \sum_{j=1}^{4} H_{jn}\, exp\left(-Im\left(z_{jn}x\right)\right.$$
$$\left. - Im(\lambda_n T_0)\right) exp\left(i(Re\left(z_{jn}x\right) + Re(\lambda_n T_0))\right)$$

It can be observed from Eq. (81) that the real part is the natural frequency and the imaginary part is the amplitude. However, a marginally negative value of the imaginary part of any of the eigenvalue (λ_n) will cause the transverse displacement ($\bar{v}$) to grow exponentially in time and this signifies the onset of the system's flutter instability.

4. Numerical Solution

This section presents the numerical solutions of the governing equations for a cantilever pipe conveying steady pressurized air/water two-phase flow under thermal loading. The air density and water density are considered as 1.225 kgm^{-3} and 1000 kgm^{-3} respectively.

4.1. Axial Natural Frequency

Equation (66) relates the flow parameters, pipe properties and the linear axial natural frequency. It can be seen from the equation that the linear axial natural frequency is independent of the effect of thermal loading, pressurization and top tension. However, variations in the flow velocities and the flexibility of the pipe will alter the linear axial natural frequencies. From equation (74), analytical solutions of the axial complex frequencies are solved for varying velocity and plotting the Argand diagram of the imaginary against the real for the various velocities, Figure 2 and 3 are obtained.

Individual velocity is considered for single phase flow while mixture velocity is considered for two phase flows. Adopting the Chisholm empirical relations as presented in equations (45) to (49), the slip ratio is estimated for the selected void fraction of 0.3 and the mixture velocity is disintegrated into the component velocities in the motion equation (66).

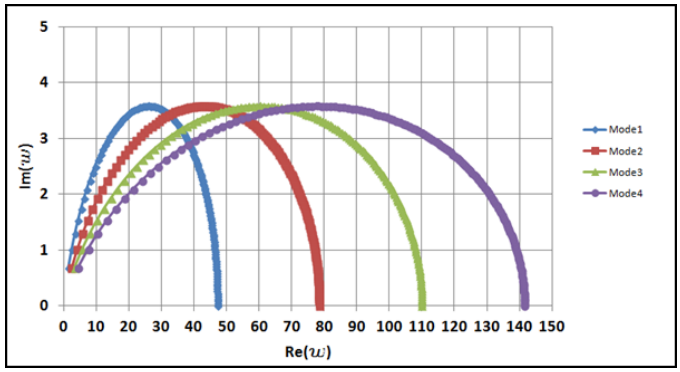

Fig. 2 First four modes axial dimensionless complex frequency as a function of dimensionless single phase flow velocity for β=0.2 and Π1=100

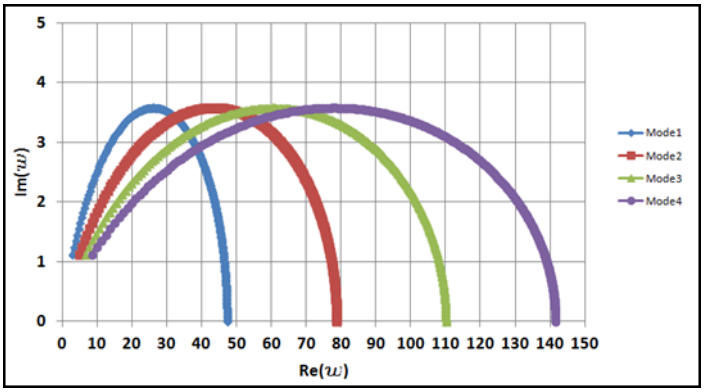

Fig. 3 First four modes axial dimensionless complex frequency as a function of dimensionless two phase flow mixture velocity for β (liquid) =0.19998, ψ (liquid) =0.9995, β (gas) =0.000105, ψ (gas) =0.0005, void fraction =0.3 and Π1=100.

For both the single phase and two phase flow, the flow velocity is used as a parametric variant gradually increasing from zero. At zero velocity, the natural frequency is that of a cantilever beam with the fluid mass as added mass. The path of the Argand diagram has a similar trend. As the fluid velocity tends towards the critical velocity; all the paths move towards the origin of the Argand diagram, which is similar to the observation by Kuiper [19].

From equation (66), the two phase flow critical velocity can be expressed as:

$$Vc = \sqrt{\frac{C5(S+1)}{C32.S^2 + C31}} \tag{83}$$

Single phase Vc can be recovered by setting S=0, which is seen to have a lesser value as compared with the two phase critical velocity.

As explained earlier, the system will be linearly unstable if the imaginary part of any of the Eigen-frequencies is less than zero. The results show that all paths possess a positive imaginary part. This signifies a stable system for flow velocities lesser than the critical velocity for a pipe discharging fluid. Comparing the Argand diagrams, it can be observed in Figure 3 that for a two phase flow the plot points cumulates to a denser plot path which signifies that more plot points are required for the convergence of the paths of the plots to the origin as compared to single phase flow in Figure 2 with sparse plot points. This observation indicates that for cantilevered pipe conveying two phase flow, the critical velocity which signifies the onset of instability is delayed and occurs at higher velocities as compared to when the pipe is conveying single phase flow.

4.2. Transverse Natural Frequency

The transverse natural frequency of the cantilever pipe as seen in equation (77) is a function of the flow parameters, pipe properties, thermal loading, pressurization and top tension. Solving the dispersive quartic equation (77) with the condition for a non-trivial solution in equation (79) simultaneously using nonlinear numerical routine written in Matlab, the complex eigenvalues are obtained.

4.2.1. The Effect of Flow Parameters

Although not the focal topic of this study, results were obtained for a simplest system with β=0.2 and Π0=Π1=Π2=0, a=αΔT=0 for a single phase flow through the pipe and compared to previous results published by Paidoussis [20] in order to demonstrate the validity of the present study.

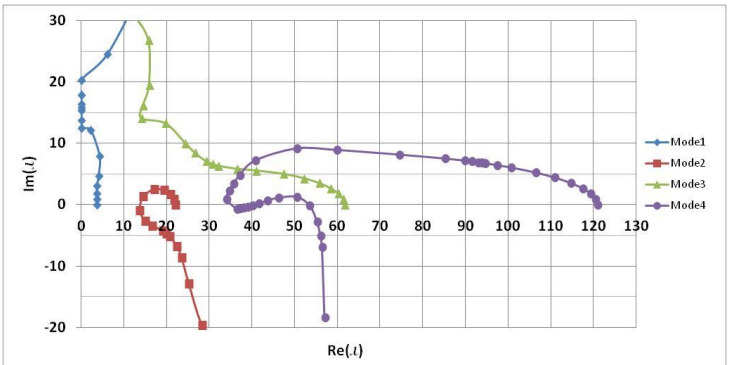

Fig. 4 First four modes transverse dimensionless complex frequency as a function of dimensionless single phase flow velocity for β=0.2 and Π0=Π1=Π2=0, a=αΔT=0

The Argand diagram presented in Figure 4 is similar to the Figure 5 obtained by Gregory & Paidoussis in 1966 as published by Paidoussis [20].

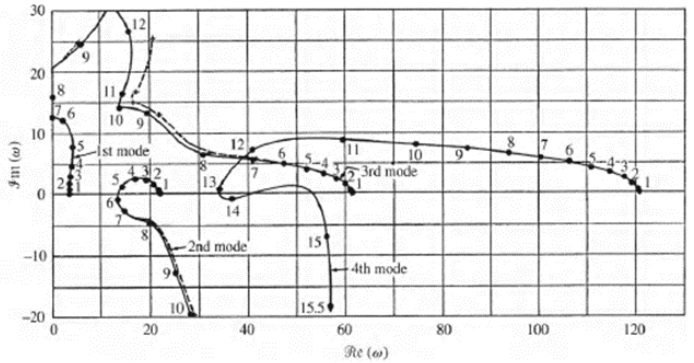

Fig 5. The dimensionless complex frequency of the four lowest modes of the cantilevered as a function of the dimensionless flow velocity, u, for β = 0.2: ——, exact analysis; – – –, four-mode Galerkin approximation [20]

Similar to the study on the axial natural frequency, the flow velocity is used as a parametric variant gradually increasing from zero. At zero velocity, the natural frequency is that of a cantilever beam with the fluid mass as added mass. However, as the velocity attains higher values, the $Im(\omega)$ in the second mode of the system starts to diminish and in time becomes negative; Therefore, a Hopf bifurcation occurs at an approximate dimensionless velocity of 5.65 which is the critical velocity at which the systems becomes transversely unstable. Also, a fourth-mode oscillatory instability is observed through Hopf bifurcation at an approximate dimensionless velocity of 13.58 as obtained by Paidoussis [20].

In this present study, various void fractions (0.1, 0.3, 0.5, 0.7 and 0.9) are considered with the corresponding slip ratios estimated from the Chisholm empirical relations presented in equations (44) and (49) the linear dynamic behavior of the two phase air and water flow is studied as follow with Π0=Π1= Π2=0, a=αΔT=0:

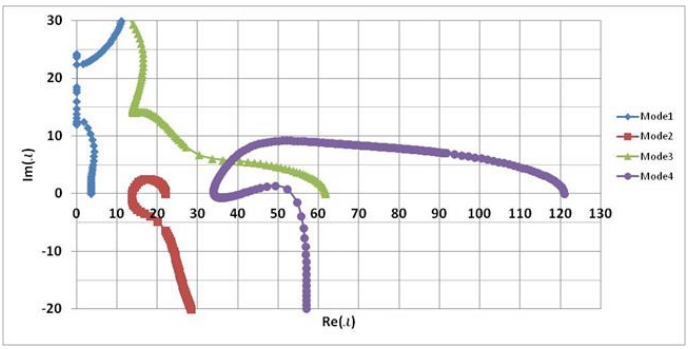

Fig. 6 First four modes transverse dimensionless complex frequency as a function of dimensionless two phase flow mixture velocity for β (liquid) =0.19999, ψ (liquid) =0.99986, β (gas) =0.0000272, ψ (gas) =0.00014, void fraction =0.1

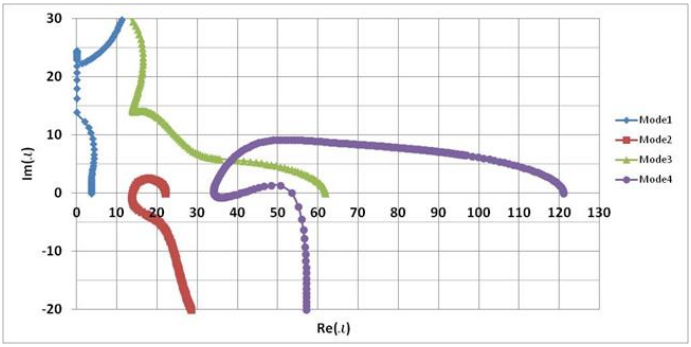

Fig. 7 First four modes transverse dimensionless complex frequency as a function of dimensionless two phase flow mixture velocity for β (liquid) =0.19998, ψ (liquid) =0.99948, β (gas) =0.000105, ψ (gas) =0.00052, void fraction =0.3

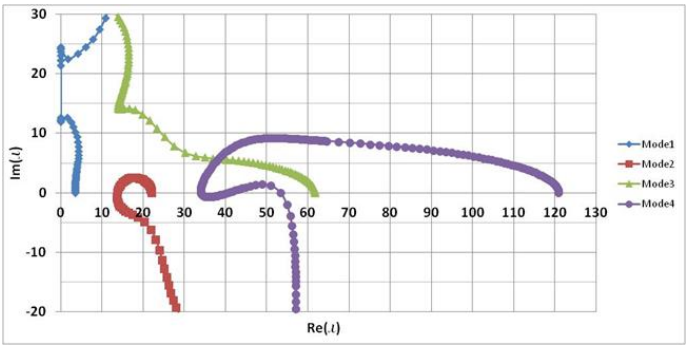

Fig 8 First four modes transverse dimensionless complex frequency as a function of dimensionless two phase flow mixture velocity for β (liquid) =0.19995, ψ (liquid) =0.99878, β (gas) =0.000245, ψ (gas) =0.00122, void fraction =0.5

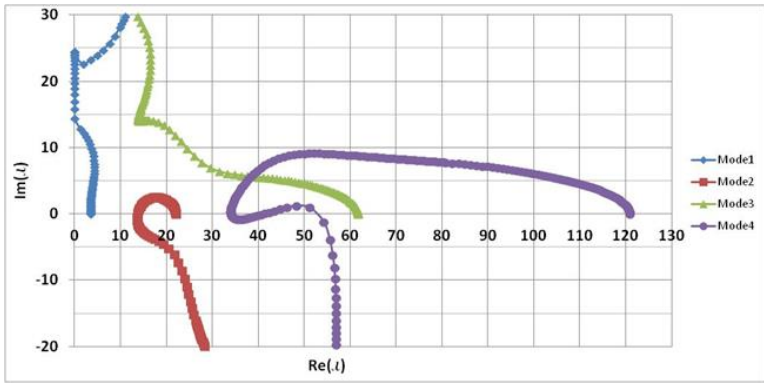

Fig. 9 First four modes transverse dimensionless complex frequency as a function of dimensionless two phase flow mixture velocity for β (liquid) =0.19989, ψ (liquid) =0.99715, β (gas) =0.0005713, ψ (gas) =0.00285, void fraction =0.7

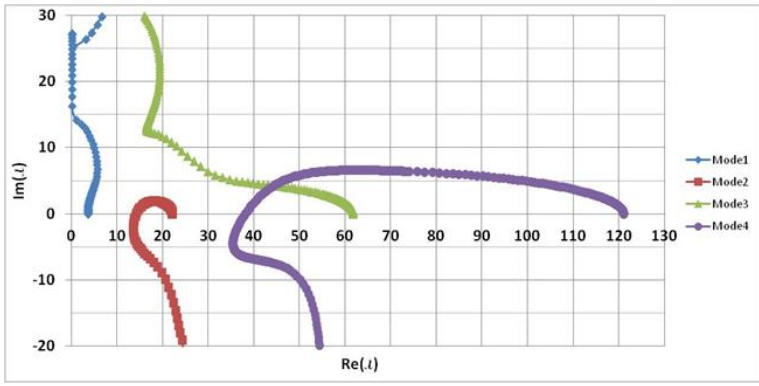

Fig. 10 First four modes transverse dimensionless complex frequency as a function of dimensionless two phase flow mixture velocity for β (liquid) =0.19956, ψ (liquid) =0.98910, β (gas) =0.0022, ψ (gas) =0.0109, void fraction =0.9.

Similar to the trend observed in Figure 4 for a single phase flow, Figure 6 to Figure 10 reveals that for the various void fractions considered, Hopf bifurcation occurred at the second mode which signifies the onset of instability transversely, the velocities at which this occurred is the critical velocity for the various void fractions. In addition, oscillatory instability is observed through Hopf bifurcation for the fourth-modes for void fractions 0.1, 0.3, 0.5 and 0.7 as revealed in Figure 6 to Figure 9, the implication of this is that for these void fractions, the fourth mode, the pipe loses stability and regains it and loses it again at some velocities. However, this did not occur in when the void fraction is 0.9 as shown in Figure 10, at the forth mode the pipe loses stability and did not regain it again.

Table 1: Summary of the dimensionless critical velocities for various void fractions

Void Fraction	Slip ratio	Dimensionless Mode 2 Hopf bifurcation velocity (Critical Velocity)	Dimensionless Mode 4 Hopf bifurcation velocity	Dimensionless Superficial critical velocity		Dimensionless critical velocity	
				Liquid	Gas	Liquid	Gas
0.1	1.057	11.502	27.392	6.213	59.104	5.592	5.910
0.3	1.237	12.505	29.782	7.988	23.046	5.591	6.914
0.5	1.616	14.613	34.804	11.173	18.053	5.587	9.026
0.7	2.685	20.382	48.524	18.436	21.216	5.531	14.851
0.9	8.351	35.338	86.671	37.791	35.065	3.779	31.559

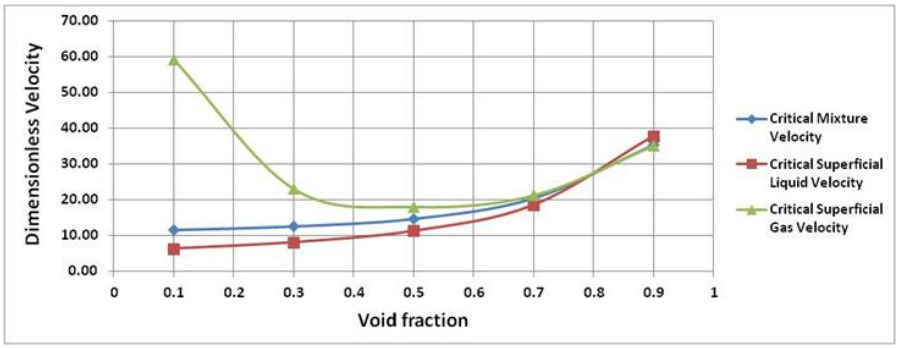

Fig. 11 Dimensionless superficial critical velocities for various void fraction

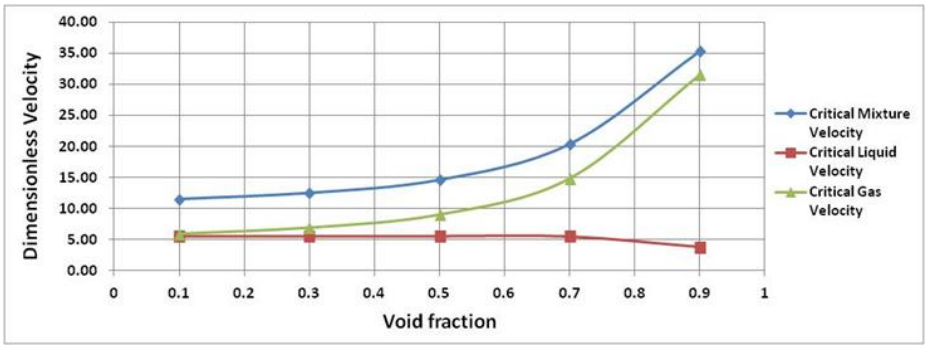

Fig. 12 Dimensionless critical velocities for various void fractions

Figure 11 and Figure 12 show that the attainment of the critical mixture velocity is delayed as the void fraction increases. Comparing the obtained critical velocity of the pipe conveying single phase flow as obtained in Figure 4 to that obtained for the various void fractions, it can be seen that the presence of the two phase flow delays the attainment of the critical velocity. This can be attributed to the fact that all the velocity dependent terms increases for a two phase flow as compared to a single phase flow (Centrifugal term and the Coriolis term). However the Coriolis term is a damping term Paidoussis [20], the additional Coriolis damping imposed by the two phase flow damps the system and makes the critical velocity of the two phase flow higher than that of a single phase flow. Also, this term increases as the void fraction increase and accounts for the increase in the value of the critical velocity as the void fraction increases.

4.2.2. The Effect of Pressurization

The effect of the pressure term is seen to make the second mode Hopf bifurcation to occur at a lower dimensionless mixture velocity of 8.238 as seen in Figure 13 as compared to the dimensionless critical mixture velocity of 12.505 obtained in Figure 7. As seen in equation (78) it is obvious that the pressure term acts similarly to the centrifugal term (MU^2) and contributes to the buckling force which hastens the onset of instability of the pipe. This observation is in line with Paidoussis [20], which highlighted that given sufficient pressurization, divergence may be induced by pressure alone.

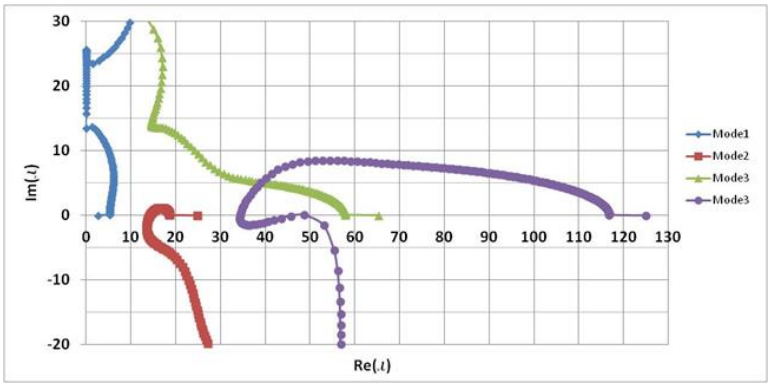

Fig. 13 First four modes transverse dimensionless complex frequency as a function of dimensionless two phase flow mixture velocity for β (liquid) =0.19998, ψ (liquid) =0.99948, β (gas) =0.000105, ψ (gas) =0.00052, void fraction =0.3, Π2 =10, Π1=Π0=a=αΔT=0

4.2.3. The Effect of Top Tension

The effect of tension term can be in two ways, depending on if it is positive or negative. A tension value less than zero indicates a compressing effect which will contributing to the buckling force in the same manner as pressurization, However, for values of tensions higher than zero as depicted in Figure 14, the observed trend is opposite to that of the pressurization effect. The positive tensioning effect is observed to have delayed the attainment of the onset of instability to a higher dimensionless mixture critical velocity of 15.637 as compared to the dimensionless critical mixture velocity of 12.505 obtained in Figure 7.

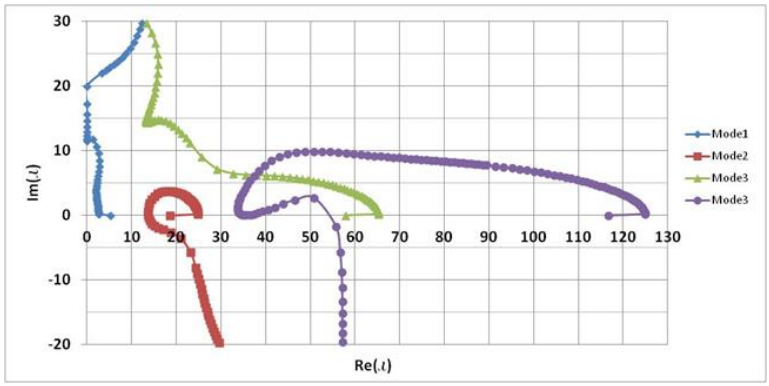

Fig. 14 First four modes transverse dimensionless complex frequency as a function of dimensionless two phase flow mixture velocity for β (liquid) =0.19998, ψ (liquid)

=0.99948, β (gas) =0.000105, ψ (gas) =0.00052, void fraction =0.3, Π0 =10, Π1=Π2=a=αΔT=0

4.2.4. The Effect of Thermal Loading

Linearly, the effect of thermal loading is akin to that of pressurisation, it can be observed from equation (78) that thermal loading term will also contribute to the buckling force and this will aid the divergence of the pipe. Figure 15 shows that the onset of instability occurred at a lower dimensionless critical velocity of 7.071 as compared to the dimensionless critical mixture velocity of 12.505 obtained in Figure 7. This corroborates the softening effect highlighted by Marakala et al [9].

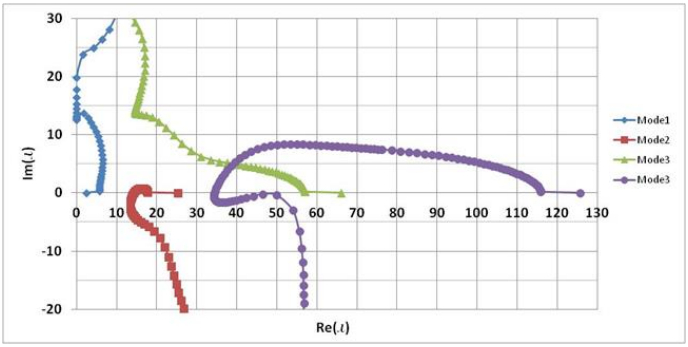

Fig. 15 First four modes transverse dimensionless complex frequency as a function of dimensionless two phase flow mixture velocity for β (liquid) =0.19998, ψ (liquid) =0.99948, β (gas) =0.000105, ψ (gas) =0.00052, void fraction =0.3, α=0.002, ΔT=60, Π1 =100, Π0=Π2=a=0

4.2.5. The Effect of Poisson Ratio

Figure 16 show that the modelling the effect of Poisson ratio delays the instability of the pipe. The dimensionless critical velocity is obtained to be 14.576 which is a higher velocity as compared to the dimensionless critical mixture velocity of 12.505 obtained in Figure 7. Also, the 4th mode Hopf bifurcation disappears with inclusion of the Poisson ratio.

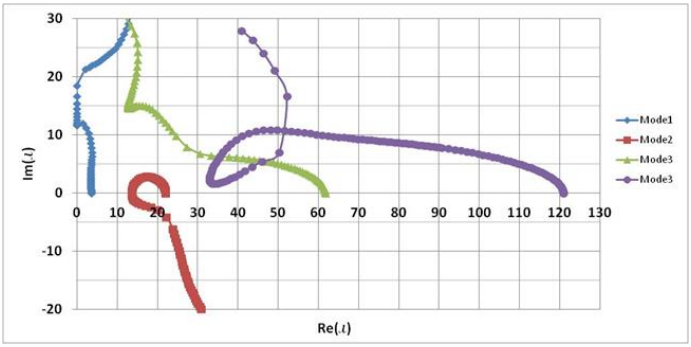

Fig. 16. First four modes transverse dimensionless complex frequency as a function of dimensionless two phase flow mixture velocity for β (liquid) =0.19998, ψ (liquid) =0.99948, β (gas) =0.000105, ψ (gas) =0.00052, void fraction =0.3, α=0, ΔT=0, Π1 = Π0=Π2=0, a=0.3.

Table 2: Summary of the effect of various parameters on critical flow velocity

Cases	Dimensionless Mode 2 Hopf bifurcation velocity (Critical Velocity)	Dimensionless Mode 4 Hopf bifurcation velocity	Dimensionless Superficial critical velocity		Dimensionless critical velocity	
			Liquid	Gas	Liquid	Gas
Mass parameters only	12.505	29.782	7.988	23.046	5.591	6.914
Effect of Pressurization	8.238	28.280	5.262	15.182	3.683	4.555
Effect of Top Tension	15.637	34.025	9.988	28.818	6.992	8.645
Effect of Thermal Loading	7.071	27.991	4.517	13.032	3.162	3.909
Effect of Poisson ratio	14.576	NA	9.310	26.862	6.517	8.059

5. Conclusion

The uniqueness and contribution of this work is the derivation of the governing equations and the study of the fluid elastic instability behaviour of extensible cantilever pipes conveying multiple phase flow as compared to previous works on pipes conveying single phase flows. This study examines the instability of a top tensioned cantilever pipe conveying pressurized two phase flow. Taking into consideration the extensible theory, nonlinear equations of motion and boundary conditions were obtained for a cantilever pipe conveying multiple phase flow using Hamilton's principle. The equations were made to be non-dimensional so as to remove the dependence on geometric and dimensional parameters. Using the method multiple scale perturbation technique, approximate solutions were obtained for a case study of a cantilever pipe conveying two phase flow of gas and liquid mixture. The leading order equation is a linear equation with the form of an undamped and unforced flow induced vibration problem. Resolution of the leading order equation resulted to the development of analytical scheme for estimating the axial and transverse natural frequencies. Numerical calculations were done to find the first four axial and transverse natural frequencies; Argand diagrams were generated for varying flow velocities. In order to assess the validity of the study, single phase results were compared with results in literature and the comparison was good. The two phase flow was modelled using the Chisholm empirical relations for various void fractions; the flow velocity was modelled as a mixture velocity accounting for the slip ratio of the phases. The axial natural frequency plot for both the single phase and two phase flow exhibits similar trends, with all the paths moving towards the origin of the Argand diagram. The velocity at which the curve intersects with the abscissa is the critical velocity of the axial vibration, which was observed to have a higher value for two phase flow as compared with the single phase flow. For the transverse natural frequencies, the Argand diagrams reveals that as the increase in flow velocity progresses gradually, a value was attained when Hopf bifurcation occurred, which is considered as the transverse vibration's critical flow velocity. The attainment of this critical flow velocity was examined for various void fractions and it was observed that the attainment of the critical velocity is delayed as the void fraction increases. A study of the effect of top tension, pressurization, thermal loading and Poisson ratio reveals that the critical velocity is attained earlier when pressurization is considered, while the effect of tension is in two ways either compressing or tensioning, a value of force less than zero will create a compression effect and acts in the same way as pressurization which aids divergence while a tensioning effect will delay the attainment of the critical velocity, the linear effect of thermal loading is akin to that of pressurisation, it hastens the attainment of the critical velocity and inclusion of the Poisson ratio in the model delays the attainment of the critical velocity of the pipe similar to the tensioning effect.

References

[1] Benjamin TB. Dynamics of a system of articulated pipes conveying fluid. I. Theory. Proceedings of the Royal Society of London. Series A. Mathematical and Physical Sciences 261; 1961:457–486. https://doi.org/10.1098/rspa.1961.0090

[2] Benjamin TB. Dynamics of a system of articulated pipes conveying fluid. II. Experiments. Proceedings of the Royal Society of London. Series A, Mathematical and Physical Sciences 261; 1961:487–499. https://doi.org/10.1098/rspa.1961.0091

[3] Gregory R W, Païdoussis M P. Unstable oscillation of tubular cantilevers conveying fluid. I. Theory, Proceedings of the Royal Society of London. Series A. Mathematical and Physical Sciences 293;1966:512–527. https://doi.org/10.1098/rspa.1966.0187

[4] Païdoussis M P, Issid N T. Dynamic stability of pipes conveying fluid. Journal of Sound and Vibration, 33(3); 1974: 267–294. https://doi.org/10.1016/S0022-460X(74)80002-7

[5] Shilling R, Lou Y K. An Experimental Study on the Dynamic Response of a Vertical Cantilever Pipe Conveying Fluid. Journal of Energy Resource Technology 102(3); 1980: 129–135. https://doi.org/10.1115/1.3227862

[6] Semler C, Li G X, Païdoussis M P. The Nonlinear Equations of Motion of Pipes Conveying Fluid. Journal of Sound and Vibration, 169; 1994:577–599. https://doi.org/10.1006/jsvi.1994.1035

[7] Ghayesh M H, Païdoussis M P, Amabili M. Nonlinear dynamics of cantilevered extensible pipes conveying fluid. Journal of Sound and Vibration, 332;2013:6405–6418. https://doi.org/10.1016/j.jsv.2013.06.026

[8] Qian Q, Lin W, Ni Q., Instability of Simply Supported Pipes Conveying Fluid under Thermal Loads. Mechanical Research Communications, 36;2009:413–417. https://doi.org/10.1016/j.mechrescom.2008.09.011

[9] Marakala N, Kuttan A K K, Kadoli R. Experimental and theoretical investigation of combined effect of fluid and thermal induced vibration on vertical thin slender tube. IOSR Journal of Mechanical and Civil Engineering, 2008:457-464.

[10] Miwa S, Mori M, Hibiki T. Two-phase flow induced vibration in piping systems. Progress in Nuclear Energy, 78; 2015:270–284. https://doi.org/10.1016/j.pnucene.2014.10.003

[11] Bai Y, Bai Q. Subsea Pipelines and Risers. Elsevier Science ISBN- 9780080445663, 2005.

[12] Monette C, Pettigrew M J. Fluid elastic instability of flexible tubes subjected to two – phase internal flow. Journal of Fluids and Structures, 19; 2004:943–956. https://doi.org/10.1016/j.jfluidstructs.2004.06.003

[13].B.G. Sinir Bifurcation and chaos of slightly curved pipes Mathematical and Computational Applications 15 (2010) 490–502. https://doi.org/10.3390/mca15030490

[14].M.A. Woldesemayat and A.J Ghajar, Comparison of void fraction correlations for different flow patterns in horizontal and upward inclined pipes International Journal of Multiphase Flow 33 (2007) 347–370. https://doi.org/10.1016/j.ijmultiphaseflow.2006.09.004

[15] Oz H R, Pakdemirli M. Vibrations of an axially moving beam with time-dependent velocity. Journal of Sound and Vibration, 227(3); 1999:239–257. https://doi.org/10.1006/jsvi.1999.2247

[16] Oz H R, Boyaci H. Transverse vibrations of tensioned pipes conveying fluid with time-dependent velocity. Journal of Sound and Vibration, 236(3); 2000:259–276. https://doi.org/10.1006/jsvi.2000.2985

[17] Oz H R, Evrensel C A. Natural frequencies of tensioned pipes conveying fluid and carrying a concentrated mass. Journal of Sound and Vibration, 250(2); 2002:368–377. https://doi.org/10.1006/jsvi.2001.3764

[18] Kesimli A, Bağdatlı S M, Çanakcı S. Free vibrations of fluid conveying pipe with intermediate support. Research on Engineering Structures and Materials, 2(2); 2016:75–87.
[19] Kuiper G L. Stability of offshore risers conveying fluid. Eburon Academic Publishers, ISBN-9789058722361,2008.
[20] Païdoussis M P. Fluid-Structure Interactions: Slender Structures and Axial Flow Vol. 1, Elsevier Academic Press, London, ISBN- 9780125443616, 2003.